Macromolecular Materials and Engineering
Open Access
www.mame-journal.de

Textile Actuators Comprising Reduced Graphene Oxide as the Current Collector

Sujan Dutta, Shayan Mehraeen, Jose G. Martinez, Tariq Bashir, Nils-Krister Persson, and Edwin W. H. Jager**

Electronic textiles (E-textiles) are made using various materials including carbon nanotubes, graphene, and graphene oxide. Among the materials here, e-textiles are fabricated with reduced graphene oxide (rGO) coating on commercial textiles. rGO-based yarns are prepared for e-textiles by a simple dip coating method with subsequent non-toxic reduction. To enhance the conductivity, the rGO yarns are coated with poly(3,4-ethylene dioxythiophene): poly(styrenesulfonic acid) (PEDOT) followed by electrochemical polymerization of polypyrrole (PPy) as the electromechanically active layer, resulting in textile actuators. The rGO-based yarn actuators are characterized in terms of both isotonic displacement and isometric developed forces, as well as electron microscopy and resistance measurements. Furthermore, it is demonstrated that both viscose rotor spun (VR) and viscose multifilament (VM) yarns can be used for yarn actuators. The resulting VM-based yarn actuators exhibit high strain (0.58%) in NaDBS electrolytes. These conducting yarns can also be integrated into textiles and fabrics of various forms to create smart e-textiles and wearable devices.

1. Introduction

Electronic textiles (e-textiles) based wearable electronic devices have gained scientific interest due to their wide range of applications such as biomedical devices,[1] sensors,[2,3] actuators,[4] storage devices,[5] and communication devices.[6] The electronic components are integrated into textiles using various methods, including sewing, twisting, knitting, and weaving.[4,7,8] E-textiles comprise electrically conductive yarns or fibers, such as metallic coated yarns,[9,10] including stainless-steel comprising yarns,[11,12] as well as conductive polymer coated yarns,[11,13] and even yarns coated with ionically conductive materials such as ionogels.[14] However, metal-based e-textiles are heavy, stiff, environmentally unstable, less corrosion resistant, and expensive.[11,12,15,16] For commercial uses, the e-textiles must be conductive as well as mechanically robust, processable, abrasion resistant, elastic, mechanically pliable, connectable, and of low weight.[17]

There are two main strategies to introduce electrical conductivity in the yarns or textiles, (1) by using metals or intrinsically conducting polymers (CPs) as filaments in the yarns and (2) by coating conventional insulating, "passive", processable yarns with conductive materials.[18] For the latter, various materials such as CPs,[19,20] CP composites,[21,22] metals,[23,24] and carbon-based materials,[25] such as carbon nanotubes,[26] carbon nanopowders,[18] and graphene[27,28] have been used. The coating strategy offers many advantages for fabricating conductive materials including adoption to existing infrastructures in the textile industry of dyeing, easy manufacturing process, low-temperature processing, low material waste, and relatively low cost.[10]

Recently, graphene has been incorporated into different polymeric materials due to its high conductivity and mechanical strength.[29–32] By adopting this concept, graphene was introduced into the textile yarns to make flexible supercapacitor electrodes, and flexible wearable physical and chemical sensors.[2,33–35] However, graphene does not coat well on common textiles because of their unfavorable interaction.[36] The oxidated form of graphene, graphene oxide (GO) is an alternative for producing textile coatings because it forms stable dispersions in polar and hydrophilic solvents allowing an efficient dipping procedure.[37,38] Subsequent reduction is needed to recover the electrical conductivity.[18,39] For example, Javed et al. reported reduced graphene oxide (rGO) on the surfaces of wool and cotton fibers to create electrically conductive networks.[37] Yun et al reported rGO/cotton yarns to enhance flexibility and electromechanical stability.[39] Cheng et al. developed a graphene-based

S. Dutta, S. Mehraeen, J. G. Martinez, E. W. H. Jager
Division of Sensor and Actuator Systems
Department of Physics
Chemistry and Biology (IFM)
Linköping University
Linköping SE-581 83, Sweden
E-mail: edwin.jager@liu.se
T. Bashir, N.-K. Persson
Polymeric E-textiles
The Swedish School of Textiles
University of Borås
Borås SE-50190, Sweden
E-mail: nils-krister.persson@hb.se

The ORCID identification number(s) for the author(s) of this article can be found under https://doi.org/10.1002/mame.202300318

DOI: 10.1002/mame.202300318

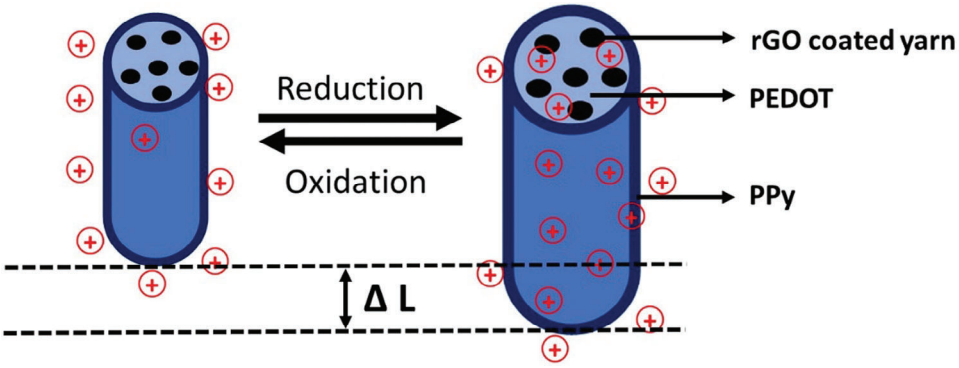

Figure 1. Mechanism of electrochemical strain of textile actuator.

fiber for sensing tensile strain, bending, and torsion.[40] Park et al. incorporated graphene nanoplatelets containing poly(4-styrene sulfonic acid) (PSS) via layer-by-layer assembly as a conductive coating on three different types of stretchable yarns.[41] Here PSS plays an important role as the aromatic rings of PSS adsorb to the graphene surface because of hydrophobic and π-π interactions. Moreover, the hydrophilic sulfonic groups of PSS prevent the agglomeration of hydrophobic graphene in polar solvents such as water. Siavashani et al. reported cotton/lycra textiles coated with ternary composites of polypyrrole (PPy), silver nanoparticles, and poly(3,4-ethylene dioxythiophene) poly(styrene sulfonate) (PEDOT:PSS) and found that PEDOT:PSS smoothens the surface.[39] Recently, our group investigated different commercial electrically conductive yarns to develop textile actuators in order to omit the initial chemical vapor phase polymerization step.[42] However, the obtained strain values were quite low ranging from ≈0.01% to 0.1%.

However, the majority of the mechanically active textile actuators exhibited relatively low electrical conductivity and low strain.[4,42] To date, there has been a lack of reported work on rGO-coated yarn with high strain due to its low conductivity on the yarn surface. So, to increase the electrical conductivity and strain, we coated the rGO-coated yarns with PEDOT:PSS. This is followed by a coating of PPy to provide the electrochemical volume changes needed to actuate the yarn. PPy undergoes reversible electrochemical oxidation and reduction in contact with the surrounding ionic species.[43,44] This results in a reversible swelling and deswelling behavior. This behavior mainly depends on the nature and size of the dopant in the PPy layer, and the ions present in the electrolyte solution.[45–51] When a PPy actuator is doped with larger anions like dodecylbenzene sulphonate (DBS^-), smaller cations present in the system will move with water and penetrate into the PPy layer resulting in elongation on reduction (Equation 1). However, when the PPy actuator is doped with smaller anions (like Cl^-), it elongates on oxidation (doping) and shortens on reduction (dedoping) and the process follows Equation 2. The mechanism of electrochemical strain is shown in **Figure 1**.

$$PPy^+(A^-) + M^+ + e^- \leftrightarrow PPy^0(A^-M^+) \quad (1)$$

$$PPy^+(a^-) + e^- \leftrightarrow PPy^0 + a^- \quad (2)$$

Here, we report scalable, conductive, flexible, and stable rGO coated viscose yarns and the use of those yarns as flexible textile actuators. Viscose yarn is a cellulose-based semi-synthetic material. Generally, cellulose is derived almost exclusively from wood pulp. Viscose is an affordable option that is generally blended with other fibers or yarns, and it is easily dyed. In our study, we used viscose rotor spun (VR) and viscose multifilament (VM) yarns with different dtex and number of filaments. First, the GO was coated on the yarn using dip coating and thereafter reduced to rGO by chemical reduction. Next, the rGO coated yarn was coated with PEDOT:PSS to ensure sufficient conductivity of the yarn and finally, a layer of the electromechanically active polypyrrole (PPy) was electropolymerized on top to produce the electroactive yarn.[42,52] The surface morphology and electrical resistance of the obtained rGO-PEDOT-PPy yarn were analyzed. The results showed successful reversible actuation of the electroactive yarns driven by an electrical voltage. In addition, we compared two different types of yarn (VR and VM) and studied their actuation behavior in detail. This new electroactive yarn could be used as a wearable linear actuator and could be woven or knitted into fabric as a wearable electrical actuator.[4]

2. Experimental Section

2.1. Materials

Viscose rotor spun (VR) Ne 30/1 yarn was purchased from Annapoorna Cotspin Co., India. Viscose multifilament (VM), dtex = 150, no of filaments = 44, yarn was purchased from Cofitex S.A, Spain. Pyrrole was purchased from Sigma, distilled under vacuum before use, and stored at -20 °C. Polyethylene glycol (PEG400), dimethyl sulfoxide (DMSO), sodium hydrosulfite (SD), and sodium dodecyl benzene sulphonate (NaDBS) were also purchased from Sigma Aldrich and used as received. PEDOT: PSS Clevios PH 1000 was obtained from Heraeus Company. To obtain the PEDOT coating solution, we mixed 20 vol% of DMSO and 10 wt.% of PEG400 in the PH 1000 PEDOT:PSS solution. In this work, PEDOT:PSS/PEG/DMSO is denoted as PEDOT in all cases unless otherwise stated. Graphene oxide (GO) was purchased from Graphenea, Spain. To prepare the GO coating solution, 400 mg of GO was dispersed in 100 mL deionized water in an ice bath using an ultrasonicator. Ultrapure

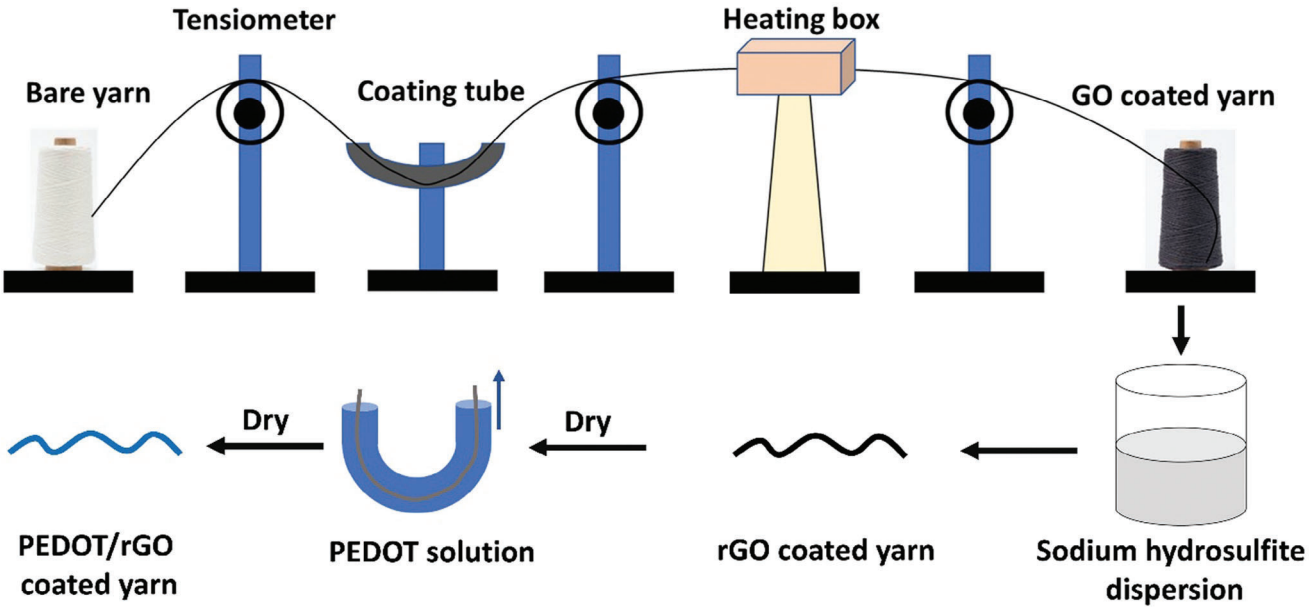

Figure 2. Fabrication of the coating setup used to dip coat and collect threads with the baths containing the coating solutions.

water (18.2 MΩ) from Millipore Milli-Q equipment was used in all experiments.

2.2. Preparation of the Conductive Yarns

For the coating process, a custom-built lab coating setup (**Figure 2**) was used. Two different viscose yarns, i.e. VR and VM, were used. The bare yarn was connected to a tensiometer, which then passed through a coating bath. After coating, the GO coated yarn was passed through a heating box to dry. Next, the dried GO coated yarn was collected manually. The yarn was coated once at a fixed speed of 1 mm/min. To convert GO to rGO, sodium dithionite was used as a reducing agent. The GO-coated yarn was dipped in sodium dithionite solution (50 mM) for 30 min at 90 °C to obtain a black coating of rGO. Next, the rGO/VR and rGO/VM coated yarns were rinsed with deionized water to remove any remaining salts and dried at 70 °C for 30 min.

After the successful completion of the dyeing, reduction, and curing process, the rGO coated yarns were coated with the PEDOT solution using a dip coating method. This second coating was applied to enhance the electrical conductivity aiming for improved actuator response. Here, 300 mm long rGO coated yarns were passed through in a U-shape pipe containing the PEDOT solution and thereafter left to dry in air for 2 h. Here, both yarns were coated 4–5 times with PEDOT:PSS solution to keep the PEDOT coating density in the range of 2–5 × 10^{-5} g mm^{-1}. However, since VM absorbed slightly more PEDOT, it showed slightly lower resistance. The density of the coated yarns was measured gravimetrically. The density was calculated at room temperature using the following equation:

$$\text{Density} = \left(W_f - W_i\right)/300 \tag{3}$$

where W_f is the mass (in grams) of the coated yarn after drying and W_i is the mass (g) of the initial uncoated yarn and 300 is the length of the yarn in mm to obtain the PEDOT mass deposited per length.

The resistance of the yarns was measured using a Multimetrix DMM220 digital multimeter over 60.00±0.01 mm yarn length by connecting hook clip test probes at the two ends. After the PEDOT coating, the rGO/VR and rGO/VM yarns were named as PEDOT/rGO/VR and PEDOT/rGO/VM. It is to be noted that the PEDOT coating density of both yarns was kept in the range of 2–5 × 10^{-5} g mm^{-1}. Hence, the strain (%) for a 20 mm electrolyte is also almost the same (Figure 8a). However, when increasing the immersion of yarns, the PPy/PEDOT/rGO/VM yarn showed more strain in comparison to the PPy/PEDOT/rGO/VR yarn. A 60 mm PPy/PEDOT/rGO/VR showed 0.16% strain (0.095 mm displacement), while PPy/PEDOT/rGO/VM showed 0.19% strain (0.114 mm displacement), i.e., a 19% increase for PPy/PEDOT/rGO/VM. This is due to the fact that PPy/PEDOT/rGO/VM was slightly more conductive as compared to PPy/PEDOT/rGO/VR.

2.3. Electropolymerization of PPy on the Conductive Yarns

Electropolymerization and cyclic voltammetry of the PEDOT/rGO/VR and PEDOT/rGO/VM coated yarns were performed in a single-compartment three-electrode electrochemical cell. The cell was connected to an Ivium CompactStat.h potentiostat (Ivium Technologies, The Netherlands) and the included Ivium software was used. The rGO/PEDOT coated yarn acted as the working electrode and was placed in the centre of the cell. Stainless steel fabric and a BASi MF-2052 Ag/AgCl (3 M NaCl) were used as the counter electrode (CE) and reference electrode (RE), respectively. The electropolymerization was performed in 0.1 M NaDBS and 0.1 M pyrrole (Py) aqueous solution by applying a constant current of 0.5 mA through the yarns for 20,000 s at room temperature. To prepare a 60 mm polypyrrole

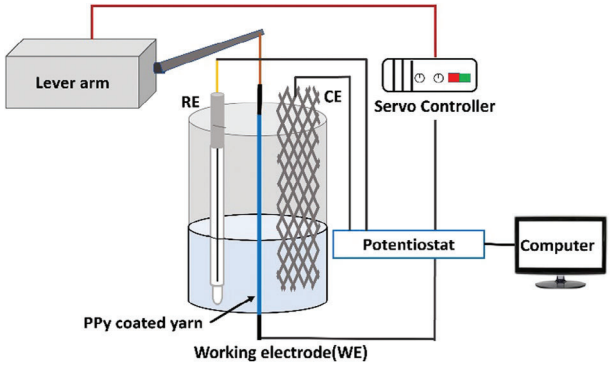

Figure 3. The experimental setup to measure the isotonic strain or isometric force.

(PPy) coated yarn, an 80 mm long PEDOT/rGO coated yarn was set as the WE electrode and the electrochemical cell was filled up to 60 mm with the polymerization solution. After successful polymerization, the yarn was rinsed with deionized water and dried at room temperature for further analysis. In this study, one fixed polymerization condition was used for all experiments since the effect of the PPy thickness had been well studied. The thickness of PPy had significant effects on the performance of the CP-based actuator.[53,54]

Cyclic voltammograms of yarns were also performed between -1.2 V and +0.2 V at 10 mV s^{-1} scan rate at room temperature using the same setup but in a 0.1 M NaDBS aqueous solution (without pyrrole monomers). After polymerization of PPy, the PEDOT/rGO/VR yarns will be denoted as PPy/PEDOT/rGO/VR and PEDOT/rGO/VM yarns will be denoted as PPy/PEDOT/rGO/VM.

2.4. Characterization

To investigate the actuation (displacement/strain and force) of the electroactive yarn, a lever arm with a servo controller (Cambridge Technology Inc. Model 200B, USA) was used (**Figure 3**). The lever arm through its associated servo controller was connected to the potentiostat analog-in port and the signal was recorded using the Nova 2.1 software of the Autolab PGSTAT204 (Metrohm Autolab) used to apply the electrical stimuli. An 80 mm electroactive yarn was firmly clamped into a single-compartment three-electrode electrochemical cell, where the upper part (10 mm) was fixed to the lever arm transducer and the lower part (10 mm) was inserted through a hole in the bottom of the cell, glued, and electrically connected using the hook clip to the WE. A stainless-steel mesh was used as CE and a BASi MF- 2052 Ag/AgCl (3 M NaCl) as RE. The lever arm settings were controlled by the lever arm servo controller and used to measure isotonic displacement/strain and isometric force, respectively.

The detailed procedure for actuation measurement is described in a previous work.[55] The isotonic strain measurement was performed at an initial preload (12.5 mN) in the 0.1 M NaDBS electrolyte solution. We have measured the strain by varying the electrolyte level. For example, a 20 mm electrolyte level means out of the 80 mm yarn length, the initial 10 mm was the mechanical contact portion, the next 40 mm was in the air, then 20 mm length of yarn was immersed into the 0.1 M NaDBS electrolyte solution, and the lower 10 mm connected through the hook clip to the WE. For the actuation study, step potentials (-1.2 V and 0.2 V) were applied to the electrochemical cell for 600 s. In the same way, the strain (%) measurements of 30, 40, 50, and 60 mm immersed yarns were done by adding the required amount of electrolyte solution in the cell. Force measurements were also done using the same setup but by changing the measurement mode of the servo controller from isotonic to isometric.

The strain (%) was calculated from the formula:

$$\text{Strain}\,(\%) = \Delta L/L * 100\% \quad (4)$$

where ΔL = displacement of the PPy coated yarn and L is the starting length of the submerged part. For example, if the yarn was immersed in a 20 mm electrolyte solution, then its L is 20 mm, and so on.[55]

All yarns were immersed in the electrolyte for 30 min before the measurement. For each measurement, three samples were prepared and measured independently. To minimize the gas evolution, we protected the metal contacts (the alligator clips). For this, the lower part (10 mm) of the yarn was inserted through a hole in the bottom of the plastic electrochemical cell and glued and sealed. The electrical contact was made by connecting the alligator clips to this short section of the yarn protruding from the cell bottom thereby avoiding any contact with the electrolyte solution. The protruding section of the yarn was coated with Ag paint to reduce the contact resistance.

The microstructure and morphology of the yarns were characterized using a scanning electron microscope (SEM, S-4800, Japan, HITACHI) with an acceleration voltage of 5 kV.

3. Results and Discussion

3.1. Fabrication of Electroactive Yarns

The schematic diagram for the fabrication of the yarns with rGO is shown in Figure 2. First, a bare yarn was coated with GO, and then it was reduced in sodium dithionite to form a rGO coated yarn. The brown colored GO coated yarn changed to black after the reduction. Next, the rGO coated yarn was coated with PEDOT from the PEDOT solution. Here, poly(4-styrenesulfonic acid) (PSS) was adsorbed onto the rGO surface because of the hydrophobic and π-π interactions. Moreover, the sulfonic groups ($-SO_3H$) of PSS also contribute to the formation of hydrogen bonds with the unreacted carboxyl groups of rGO.[42] The PEDOT coating was confirmed by comparing with the resistance of the rGO coated yarns with that of the PEDOT coated yarns. The resistance of PEDOT/rGO/VR and PEDOT/rGO/VM were ≈140 Ω cm^{-1}, and ≈110 Ω cm^{-1}, respectively, whereas both rGO coated yarns showed very high resistance (≈27 kΩ cm^{-1}). Finally, to deposit a layer of PPy on PEDOT/rGO yarn, electropolymerization was performed in a single-compartment three electrode electrochemical cell. The results of rGO coated and PEDOT/rGO coated yarns are summarized in **Table 1**.

The characteristic curves of the electrochemical deposition of PPy on the PEDOT/rGO coated yarns and the corresponding CV curves are shown in **Figure 4**. The PPy coatings on

Table 1. Specifications of rGo and rGO/PEDOT coated yarns.

Yarn	Resistivity	No. of Coatings
rGO/VR	≈27 kΩ cm^{-1}	1[a)]
PEDOT/rGO/VR	≈140 Ω cm^{-1}	4,5[b)]
rGO/VM	≈27 kΩ cm^{-1}	1[a)]
PEDOT/rGO/VM	≈110 Ω cm^{-1}	4,5[b)]

[a)] No of rGO coatings on VR and VM yarns; [b)] No of PEDOT coatings on rGO/VR and rGO/VM yarns.

Table 2. Reversible and irreversible consumed charge during actuation of rGO, rGO/PEDOT, and PPy/rGO/PEDOT coated yarns.

Sample name	Reversible charge [mC]	Irreversible charge [mC]
rGO/VR	0.25	0.84
PEDOT/rGO/VR	2.49	5.09
PPy/PEDOT/rGO/VR	18.26	38.18
rGO/VM	0.25	0.84
PEDOT/rGO/VM	2.82	5.19
PPy/PEDOT/rGO/VM	19.69	53.01

both yarns were obtained in 0.1 M NaDBS and 0.1 M pyrrole aqueous solution by applying a constant current of 0.5 mA for 20 000 s at room temperature. It can be seen in Figure 4a that initially the potential increased then decreased, and finally reached a steady potential, which indicates the uniform deposition of PPy on the PEDOT/rGO coated yarns.[52] However, the potential developed for PPy/PEDOT/rGO/VR was higher (0.68 V) than PPy/PEDOT/rGO/VM (0.58 V). This can be explained as PPy/PEDOT/rGO/VM yarns were more conductive in comparison to PPy/PEDOT/rGO/VR yarns (Table 1), which lowered the potential needed to drive the electrochemical synthesis.

To confirm the electroactivity after PPy coating, the cyclic voltammetry of the rGO, PEDOT/rGO, and PPy/PEDOT/rGO coated yarns were also carried out in 0.1 M NaDBS aqueous solution between -1.2 V and +0.2 V versus Ag/AgCl at room temperature. Figure 4b,c show the corresponding cyclic voltammograms for PPy, PEDOT, and rGO coated VR and VM yarns respectively. After PEDOT coating, PEDOT/rGO/VR yarn showed higher current compared to rGO/VR yarn, including the typical redox peaks for PEDOT. Moreover, PPy/PEDOT/rGO/VR yarn showed a sixfold higher current compared to PEDOT/rGO/VR yarn and the typical PPy redox peaks. Thus, it can be concluded that after PPy synthesis, a good PPy deposition was achieved on PEDOT/rGO/VR yarns and PPy was the main source of the electroactivity. Similar observations were also found for VM yarn. Also, here, PPy/PEDOT/rGO/VM yarn showed higher current in comparison to rGO/VM and PEDOT/rGO/VM yarns.

We have also calculated the reversible and irreversible consumed charge (C) of rGO, rGO/PEDOT, and PPy/rGO/PEDOT coated yarns and the data shown in **Table 2**. As can be seen (Figure S2, Supporting Information), by adding PEDOT and PPy layers the consumed charge per cycle has increased which is attributed to the thickness of the CP layers. The reversible charge for PPy/PEDOT/rGO/VR was 18.26 mC, whereas the irreversible charge was 38.18 mC. However, the reversible charge for PPy/PEDOT/rGO/VM was 19.69 mC, whereas the irreversible charge was 53.01 C, which is higher than the PPy/PEDOT/rGO/VR. The irreversible charges could be due to hydrogen evolution, but we did not see any hydrogen (bubble) generation, or oxidation of the silver paint used to reduce the contact resistance between the yarn protruding from the electrochemical cell and alligator clip.

3.2. Surface Morphology

After the different coatings, SEM images were taken (**Figure 5**). They confirm the successful deposition of rGO, PEDOT, and PPy onto the viscose rotor spun and viscose multi-filament yarns. The SEM images show that after rGO coating, the yarn was not totally covered or filled with rGO, while PEDOT was able to fill the gaps between the filaments, thus making the surface smoother and increasing the conductivity. After PPy polymeriation, a uniform coating of PPy was achieved along the yarn. A better filling after PEDOT coating was achieved due to the interaction of -OH functional groups of rGO with the -PSS functional groups of PEDOT. The high magnification images of the PPy-coated yarns show a uniform coating (Figure 5c1 and 5f1).

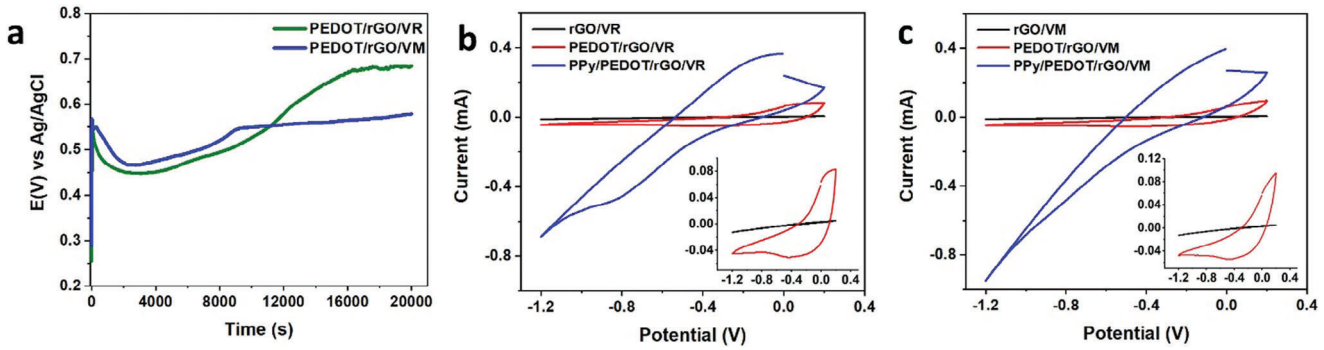

Figure 4. Electrochemical responses of the different yarns. a) Potential generated during electrochemical polymerization of PPy on PEDOT/rGO/VR and PEDOT/rGO/VM yarns in a three-electrode cell (galvanostatic, 0.5 mA, 20000 s) in a 0.1 M Py, 0.1 M NaDBS solution. Cyclic voltammograms of b) rGO/VR, PEDOT/rGO/VR, PPy/PEDOT/rGO/VR c) rGO/VM, PEDOT/rGO/VM, PPy/PEDOT/rGO/VM yarns in 0.1 M NaDBS solution between −1.2 V and +0.2 V versus Ag/AgCl at room temperature.

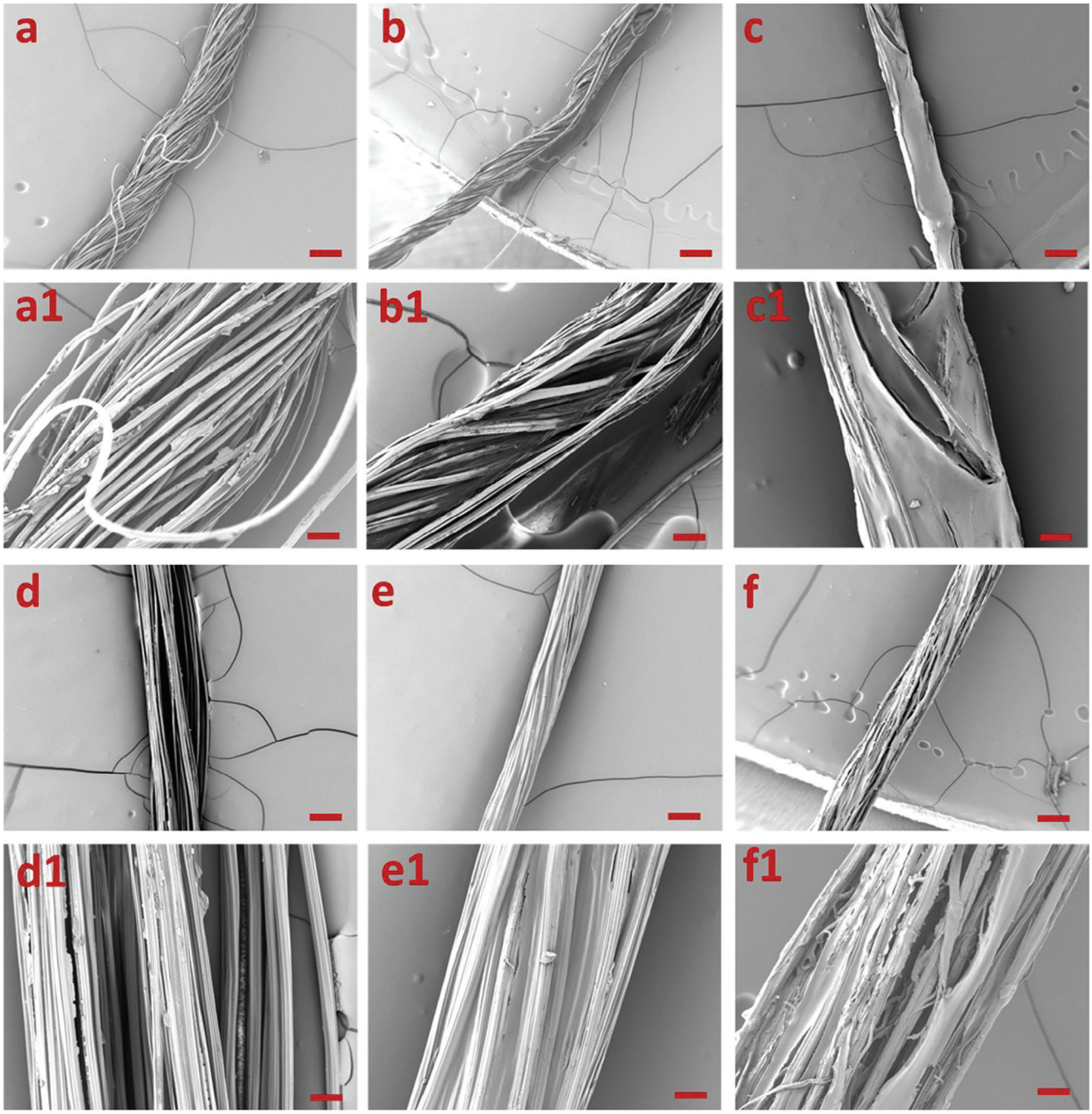

Figure 5. SEM images of viscose rotor spun yarns a) rGO/VR b) PEDOT/rGO/VR and c) PPy/PEDOT/rGO/VR yarn d) rGO/VM e) PEDOT/rGO/VM and f) PPy/PEDOT/rGO/VM yarn at 100× magnification, Scale bar: 200 µm (above) and the corresponding images (a1, b1,c1, d1,e1, and f1) at: 500× magnification, Scale bar: 50 µm (below).

3.3. Linear Actuation Measurement

In order to investigate the linear actuation of the different yarns, we performed isotonic strain measurements using a square potential wave of −1.2 V to +0.2 V versus Ag/AgCl for 10 cycles in 0.1 M NaDBS electrolyte at an applied constant load of 12.5 mN. Yarns coated with only rGO or PEDOT showed very little actuation during oxidation/reduction of a 40 mm immersed yarn (Figure S1, Supporting Information). This is due to the rGO not being a good electromechanically active material.

Figure 6 shows the actuation for PPy/PEDOT/rGO/VR and PPy/PEDOT/rGO/VM yarns during square wave potential step oxidation/reduction in 0.1 M NaDBS electrolyte solution in the potential range −1.2 V to +0.2 V under 12.5 mN load. Both types of yarn show quite similar movement (contraction/expansion), i.e. reversible contraction during oxidation and reversible expan-

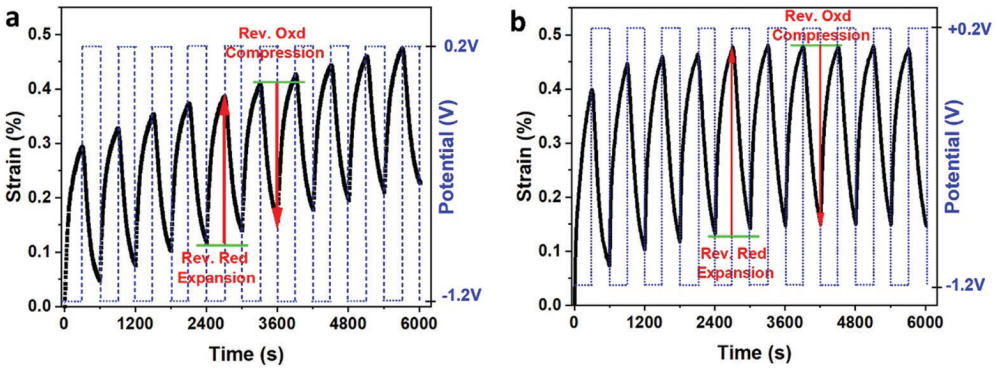

Figure 6. Strain measurements using a square wave potential for a) PPy/PEDOT/rGO/VR and b) PPy/PEDOT/rGO/VM for 10 cycles in 0.1 M NaDBS solution in potential range −1.2 V to +0.2 V under 12.5 mN load. The length of the active portion is 40 mm.

sion during reduction. The movement can be explained as the exchange of cations (Na^+), according to electrochemical reaction (1). The upward part of the curve in Figure 6 represents the expansion (reduction) when Na^+ ions migrate from the solution into the PPy layer. The downward curve represents the contraction (oxidation) when Na^+ cations are expelled from the PPy layer.[25] However, the expansion and contraction peaks were higher in case of PPy/PEDOT/rGO/VM yarn (0.30%) as compared to PPy/PEDOT/rGO/VR yarn (0.26%). We attribute this to the higher conductivity of the PEDOT/rGO/VM yarn (Table 1). Also, the actuation became stable after already 4 cycles for the VM textile actuator, while this is not the case for the VR yarn.

The effect of electrolyte level on the strain measurement is shown in **Figure 7**a,b. A series of experiments have been performed to see the electrochemical actuation of the yarn immersed in the electrolyte solutions. The maximum electrochemical strain for PPy/PEDOT/rGO/VR yarn was 0.58% for a 20 mm submerged length. The electrochemical strain was decreased with increasing the submerged length yarn and the values for 30, 40, 50, and 60 mm active yarn showed 0.38%, 0.26%, 0.22%, and 0.16%, respectively. We also measured the strain for PPy/PEDOT/rGO/VM yarn and found quite similar observations to PPy/PEDOT/rGO/VR yarn. The maximum strain of PPy/PEDOT/rGO/VM for 20, 30, 40, 50, and 60 mm immersed

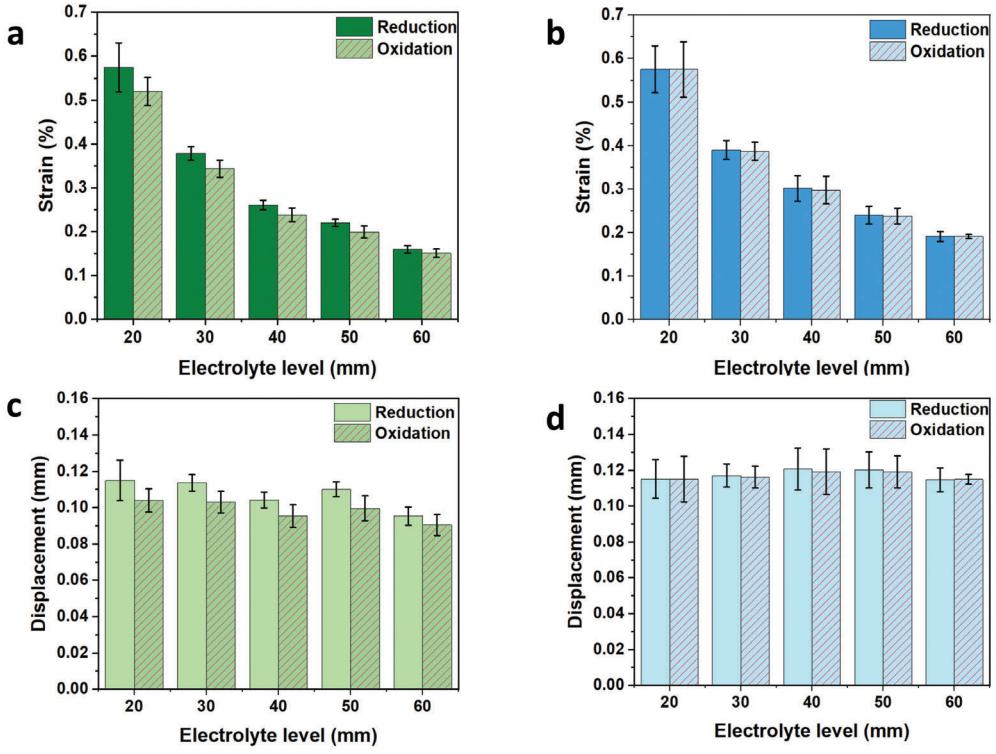

Figure 7. Measured strain (%) as a function of electrolyte level for a) PPy/PEDOT/rGO/VR and b) PPy/PEDOT/rGO/VM. Displacement for c) PPy/PEDOT/rGO/VR and d) PPy/PEDOT/rGO/VM.

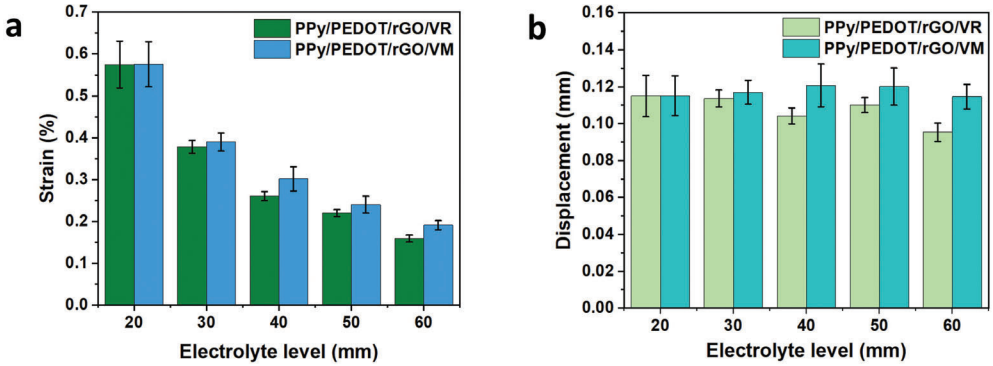

Figure 8. Actuation comparison of PPy/PEDOT/rGO/VR and PPy/PEDOT/rGO/VM yarns: a) strain (%), b) displacement comparison (reduction value) (reorganized from Figure 7).

in the electrolyte were 0.57%, 0.38%, 0.30%, 0.24%, and 0.19%, respectively.

The displacement for both PPy/PEDOT/rGO/VR (Figure 7c) and PPy/PEDOT/rGO/VM (Figure 7d) was also measured. For PPy/PEDOT/rGO/VR yarn the displacement was slightly decreased with increasing electrolyte level and after 40 mm, it became constant. However, the displacement values for PPy/PEDOT/rGO/VM were almost the same throughout the active yarn lengths. The reduction of the strain at increasing electrolyte levels can be explained as the strain value is calculated as $\Delta L/L^* 100\%$, where ΔL is the displacement of the PPy coated yarn and L is the electrolyte level. Since the value of the displacement ΔL was almost the same throughout the electrolyte levels, L, the reduction of the strain value was a consequence of how the strain is calculated. If L increases, but ΔL remains constant, $\Delta L/L^* 100\%$ will be decreased. This indicates that only a short portion of the yarn (<20 mm) was electro-mechanically active as we have noticed previously.[55]

Figure 8 shows the isotonic strain (a) and displacement (b) compared between PPy/PEDOT/rGO/VR and PPy/PEDOT/rGO/VM yarns. (Reorganised from Figure 7 and only the strain (%) and displacement during reduction to easier compare the two cases.) As it can be seen, the 20 mm immersed yarns showed almost the same strain. However, when increasing the immersion of yarns, the PPy/PEDOT/rGO/VM yarn showed more strain in comparison to PPy/PEDOT/rGO/VR yarn. A 60 mm PPy/PEDOT/rGO/VR showed 0.16% strain (0.095 mm displacement), while PPy/PEDOT/rGO/VM showed 0.19% strain (0.114 mm displacement), i.e., a 19% increase for PPy/PEDOT/rGO/VM.

3.4. Force Measurement

The isometric force generation during redox cycling was measured in a 30 mm electrolyte level with the applied potential varied between −1.2 V and +0.2 V (**Figure 9**). A reversible force of 28.2 mN was generated for a 30 mm PPy/PEDOT/rGO/VR single yarn. In addition to the reversible isometric force, a drift was present, visible as a negative slope. This is due to the pre-stretching that causes a stress relaxation transient, which is also seen by others.[56] However, in the case of strain (%), pre-stretching implies a creep transient and shows a positive slope drift. Figure 9b shows the developed isometric forces (mN) for PPy/PEDOT/rGO/VM yarn, in which the generated force is 38.55 mN for a 30 mm single yarn. However, the creep behavior remained same for both yarns.

Next, we studied the effect of the electrolyte level of yarn on force measurement. As can be seen in **Figure 10**a, the developed isometric force for PPy/PEDOT/rGO/VR yarn was decreased

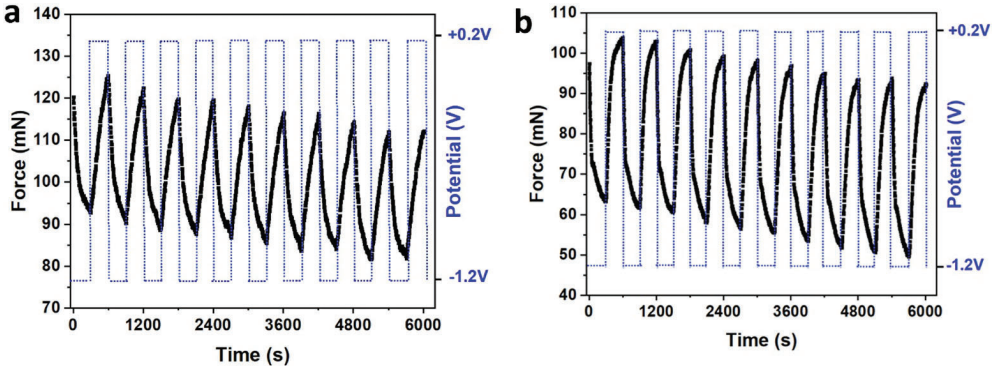

Figure 9. Developed Isometric forces (mN) of the actuator versus time (s) for a) PPyPPy/PEDOT/rGO/VR and b) PPy/PEDOT/rGO/VM for 10 cycles in 0.1 M NaDBS solution under 150 mN load. The submerged length is 30 mm.

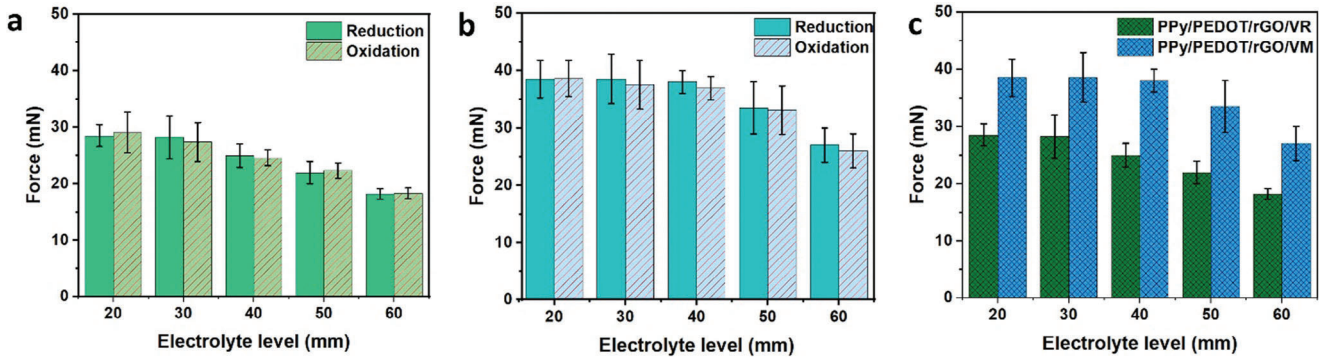

Figure 10. Developed isometric forces for a) PPy/PEDOT/rGO/VR b) PPy/PEDOT/rGO/VM. c) comparison of isometric developed forces (reduction value) as a function of the electrolyte level (reorganized from 10 a and b).

with increasing the submerged length yarn and the values for 20, 30, 40, 50, and 60 mm active yarn showed 28.5, 28.2, 24.9, 21.9, and 18.2 mN, respectively. For PPy/PEDOT/rGO/VM, the yarn showed a similar decrease in force with increasing electrolyte levels (Figure 10b). The maximum forces of PPy/PEDOT/rGO/VM for 20, 30, 40, 50, and 60 mm immersed in the electrolyte were 38.5, 38.6, 38, 33.5, and 27 mN, respectively.

The comparison of isometric force between PPy/PEDOT/rGO/VR and PPy/PEDOT/rGO/VM yarns is shown in Figure 10c. It can be seen that PPy/PEDOT/rGO/VM yarn generated more force as compared to PPy/PEDOT/rGO/VR yarn. For instance, the force for a 20 mm active of PPy/PEDOT/rGO/VR is 28.5 mN and PPy/PEDOT/rGO/VM is 38.5 mN, thus showing a 35% increase for PPy/PEDOT/rGO/VM yarn. This high difference in generated force is attributed to the higher conductivity of PPy/PEDOT/rGO/VM yarn as compared to PPy/PEDOT/rGO/VR.

We also plotted charge versus time curves for the two samples. **Figure 11**a shows the comparison of consumed charge during the strain measurement for one of the replicates that are shown in Figure 6a,b as an example. Similarly, Figure 11b shows the comparison of the consumed charge during the force measurements for one of the replicates that are shown in Figure 10c of the manuscript as an example. For a 40 mm submerged length, both PPy/PEDOT/rGO/VR and PPy/PEDOT/rGO/VM transferred a similar charge. This observation was also found when we plotted the charge (C) versus electrolyte level (Figure 11c). With increasing electrolyte levels, the consumed charge also increased until 40 mm, and after that it becomes constant. In most of the cases, we found that the consumed charge in the case of PPy/PEDOT/rGO/VM is larger than PPy/PEDOT/rGO/VR, which explains why the PPy/PEDOT/rGO/VM yarn has a larger displacement. Also, the consumed charge (C) versus electrolyte level shows the same trend as the strain and force versus electrolyte level which supports the conclusion that indeed the plateau seen in the strain and force data is caused by the iR drop.

4. Conclusion

Here, we reported a textile actuator fabricated by simple coating with rGO and PEDOT, followed by PPy electropolymerization, which is a facile, cost-effective way to produce soft actuators. rGO can be applied on two types of viscose yarn (VM and viscose rotor spun). After PEDOT coating the resistance of the rGO coated yarns (27 kΩ cm^{-1}) was reduced to ≈140 Ω cm^{-1}, and ≈110 Ω cm^{-1} for PEDOT/rGO/VR and PEDOT/rGO/VM respectively. Next, we demonstrated that such rGO coated yarns can be used to make soft actuators, i.e., electroactive textile actuators. The actuator yarns were characterized electrochemically and using electron microscopy as well as both isotonic

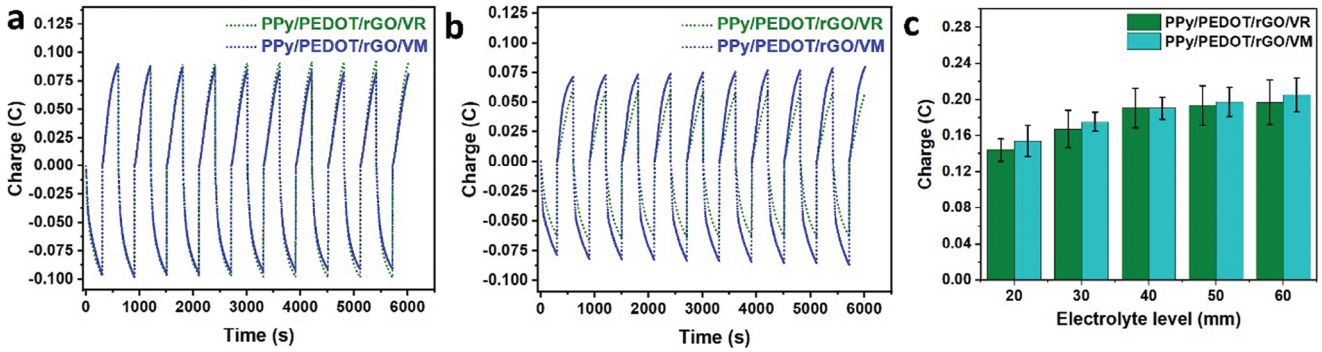

Figure 11. Charge (C) measurements using a square wave potential for PPy/PEDOT/rGO/VR and PPy/PEDOT/rGO/VM during a) strain and b) force measurements for 10 cycles in 0.1 M NaDBS solution in the potential range −1.2 V to +0.2 V under 12.5 mN load for 40 mm electrolyte level. c) Comparison of the consumed charge of PPy/PEDOT/rGO/VR and PPy/PEDOT/rGO/VM yarns during strain measurement (during reduction half cycle) for various electrolyte levels (submerged lengths).

displacement and isometric developed forces. SEM images confirmed the uniform deposition of PPy along the yarns. Both PPy/PEDOT/rGO/VR and PPy/PEDOT/rGO/VM yarns showed good electrochemical strains of 0.58% and 0.57%. The force for a 20 mm active yarn of PPy/PEDOT/rGO/VR was 28.5 mN and of PPy/PEDOT/rGO/VM was 38.5 mN, thus showing a 35% increase for the PPy/PEDOT/rGO/VM yarn, which we contribute to higher conductivity of the coated VM yarn. Our study shows that rGO also is an interesting material to use as a (first) conductive coating layer to make conductive yarns and textile actuators. This opens thus new perspectives in the development of textile yarns with enhanced conductivity and/or actuation with possible applications in the field of smart textile materials.

Supporting Information

Supporting Information is available from the Wiley Online Library or from the author.

Acknowledgements

The authors acknowledge the Erling-Persson Family Foundation (grant no 202-00054), the Promobilia Foundation (grant no. A21029), and European Union's Horizon 2020 research and innovation program under grant agreement no. 825232 "WEAFING" for their financial support.

Conflict of Interest

The authors declare no conflict of interest.

Data Availability Statement

The data that support the findings of this study are available from the corresponding author upon reasonable request.

Keywords

actuator, e-textiles, graphene oxide, strain, viscose multifilament, viscose rotor spun

Received: September 6, 2023
Revised: October 31, 2023
Published online:

[1] F. Carpi, D. Derossi, *IEEE Tran Info. Technol. Biomed.* **2005**, *9*, 295.
[2] D. Du, P. Li, J. Ouyang, *J. Mater. Chem. C* **2016**, *4*, 3224.
[3] A. Kapoor, M. McKnight, K. Chatterjee, T. Agcayazi, H. Kausche, A. Bozkurt, T. K. Ghosh, *Adv. Mat. Tech.* **2019**, *4*,800281.
[4] A. Maziz, A. Concas, A. Khaldi, J. Stålhand, N.-K. Persson, E. W. H. Jager, *Sci. Adv.* **2017**, *3*, 1600327.
[5] X. Li, X. Chen, Z. Jin, P. Li, D. Xiao, *Mater. Chem. Front.* **2021**, *5*, 1140.
[6] T. F. Kennedy, P. W. Fink, A. W. Chu, N. J. Champagne, G. Y. Lin, M. A. Khayat, *IEEE Trans. Antennas Propag.* **2009**, *57*, 910.
[7] S. Seyedin, J. M. Razal, P. C. Innis, A. Jeiranikhameneh, S. Beirne, G. G. Wallace, *ACS Appl. Mater. Interfaces* **2015**, *7*, 21150.
[8] Y. Wang, J. Qiao, K. Wu, W. Yang, M. Ren, L. Dong, Y. Zhou, Y. Wu, X. Wang, Z. Yong, J. Di, Q. Li, M. Horiz, **2020**, *7*, 3043.
[9] W. Root, T. Wright, B. Caven, T. Bechtold, T. Pham, *Polymers* **2019**, *11*, 784.
[10] Y. J. Yun, C. Seong, W. G. Hong, H. J. Kim, J. Shind, Y. Jun, *Nanoscale* **2017**, *9*, 11439.
[11] L. M. Castano, A. B. Flatau, *Smart Mater. Struct.* **2014**, *23*, 053001.
[12] E. R. Post, M. Orth, P. R. Russo, N. Gershenfeld, *IBM Syst. J.* **2000**, *39*, 840.
[13] Z. Li, Z. Liu, H. Sun, C. Gao, *Chem. Rev.* **2015**, *115*, 7046.
[14] C. Huniade, D. Melling, C. Vancaeyzeele, G. T.-M. Nguyen, F. Vidal, C. Plesse, E. W. H. Jager, T. Bashir, N.-K. Persson, *Adv. Mater. Technol.* **2022**, *7*, 2101692.
[15] H. Li, W. Mirihanage, A. D. Smith, J. Donoghue, A. Fernando, *Mat. Lett.* **2020**, *273*, 127948.
[16] W. Zeng, L. Shu, Q. Li, S. Chen, F. Wang, X.-M. Tao, *Adv. Mat.* **2014**, *26*, 5310.
[17] S. Afroj, N. Karim, Z. Wang, S. Tan, P. He, M. Holwill, D. Ghazaryan, A. Fernando, K. S. Novoselov, *ACS Nano* **2019**, *13*, 3847.
[18] K. Chatterjee, J. Tabor, T. K. Ghosh, *Fibers* **2019**, *7*, 51.
[19] X. Ye, Z. Yuan, H. Tai, W. Li, X. Du, Y. Jiang, *J. Mater. Chem. C* **2017**, *5*, 7746.
[20] Y. Song, S. Zhou, K. Jin, J. Qiao, Da Li, C. Xu, D. Hu, J. Di, M. Li, Z. Zhang, Q. Li, *Nanoscale* **2018**, *10*, 4077.
[21] J. Xiong, J. Chen, P. S. Lee, *Adv. Mat.* **2021**, *33*, 2002640.
[22] S. Aziz, J. G. Martinez, B. Salahuddin, N.-K. Persson, E. W. H. Jager, *Adv. Funct. Mat.* **2021**, *31*, 2008959.
[23] Z. Tang, D. Yao, D. Du, J. Ouyang, *Journal of Mat. Chem. C* **2021**, *8*, 2741.
[24] S. Aziz, J. G. Martinez, J. Foroughi, G. M. Spinks, E. W. H. Jager, *Macromol. Mater. Eng.* **2020**, *305*, 2000421.
[25] I. Chodak, M. Omastova, J. Pionteck, *J. Appl. Polym. Sci.* **1903**, *82*, 2001.
[26] A. Fernando, S. Ali, S. Tan, G. He, *Proceedings* **2020**, *32*, 21.
[27] S. Afroj, S. Tan, A. M. Abdelkader, K. S. Novoselov, N. Karim, *Adv. Funct. Mat.* **2020**, *30*, 2000293.
[28] N. Karim, S. Afroj, S. Tan, K. S. Novoselov, S. G. Yeates, *Sci. Rep.* **2019**, *9*, 8035.
[29] L. Maneval, B. Atawa, A. Serghei, N. Sintes-Zydowicz, E. Beyou, *J. Mater. Chem. C* **2021**, *9*, 14247.
[30] A. K. Geim, *Science* **2009**, *324*, 1530.
[31] A. Pazat, C. Barrès, F. Bruno, C. Janin, E. Beyou, *Polym. Rev.* **2018**, *58*, 403.
[32] L. Ripoll, C. Bordes, P. Marote, S. Etheve, A. Elaissari, H. Fessi, *Colloids Surf., A* **2012**, *397*, 24.
[33] S. Bhattacharjee, R. Joshi, A. A. Chughtai, C. R. Macintyre, *Adv. Mat. Interfaces* **2019**, *6*, 1900622.
[34] X. Li, T. Hua, B. Xu, *Carbon* **2017**, *118*, 686.
[35] M. Zhang, C. Wang, Qi Wang, M. Jian, Y. Zhang, *ACS Appl. Mater. Interfaces* **2016**, *8*, 20894.
[36] D. Kowalczyk, W. Fortuniak, U. Mizerska, I. Kaminska, T. Makowski, S. Brzezinski, E. Piorkowska, *Cellulose* **2017**, *24*, 4057.
[37] K. Javed, C. M. A. Galib, F. Yang, C.-M. Chen, C. Wang, *Synth. Met.* **2014**, *193*, 41.
[38] A. Chatterjee, M. Nivas Kumar, S. Maity, *J. Text. Inst.* **2017**, *108*, 1910.
[39] Y. J. Yun, H. J. Lee, T. H. Son, H. Son, Y. Jun, *Compos. Sci. Technol.* **2019**, *184*, 107845.
[40] Y. Cheng, R. Wang, J. Sun, L. Gao, *Adv. Mat.* **2015**, *27*, 7365.
[41] J. J. Park, W. J. Hyun, S. C. Mun, Y. T. Park, O. O. Park, *ACS Appl. Mater. Interfaces* **2015**, *7*, 6317.
[42] J. G. Martinez, K. Richter, N.-K. Persson, E. W. H. Jager, *Smart Mater. Struct.* **2018**, *27*, 074004.
[43] E. W. H. Jager, E. Smela, O. InganaS, *Science* **2000**, *290*, 1540.
[44] E. Smela, *J. Micromech. Microeng.* **1999**, *9*, 1.

[45] Q. Pei, O. Inganaes, *J. Phys. Chem.* **1992**, *96*, 10507.
[46] Q. Pei, O. Inganas, *Solid State Ionics* **1993**, *60*, 161.
[47] S. Hara, T. Zama, S. Sewa, W. Takashima, K. Kaneto, **2003**, *32*, 576.
[48] S. Hara, T. Zama, W. Takashima, K. Kaneto, *Polym. J.* **2004**, *36*, 151.
[49] T. Nakashima, D. Kumar, W. Takashima, T. Zama, S. Hara, S. Sewa, K. Kaneto, *Curr. Appl. Phys.* **2005**, *5*, 202.
[50] T. F. Otero, G. Vázquez Arenas, J. J. López Cascales, *Macromolecules* **2006**, *39*, 9551.
[51] T. F. Otero, J. G. Martinez, *Chem. Mater.* **2012**, *24*, 4093.
[52] J. Foroughi, G. M. Spinks, S. Aziz, A. Mirabedini, A. Jeiranikhameneh, G. G. Wallace, M. E. Kozlov, R. H. Baughman, *ACS Nano* **2016**, *10*, 9129.
[53] D. Melling, S. Wilson, E. W. H. Jager, *Smart Mater. Struct.* **2013**, *22*, 104021.
[54] S. Hara, T. Zama, W. Takashima, K. Kaneto, *Synth. Met.* **2004**, *146*, 47.
[55] S. Dutta, S. Mehraeen, N.-K. Persson, J. G. Martinez, E. W. H. Jager, *Sens Actuators B Chem* **2022**, *370*, 132384.
[56] A. Della Santa, D. De Rossi, A. Mazzoldi, *Synth. Met.* **1997**, *90*, 93.